"Measurement and Control of Current Waveform in an Ablative Z-Pinch Pulsed Plasma Thruster"

Reducing Current Ringing in the AZPPT2 Circuit

Abstract

The second Ablative Z-Pinch Pulsed Plasma Thruster (AZPPT2) is a 2.5kg device employing a recent electromagnetic propulsion design to achieve specific impulses of 468s. The magnetic field induced by the current-carrying Teflon plasma causes the current to contract towards the axis of symmetry of the cylindrical device, effectively squeezing the Teflon particles out the exhaust hole at highly accelerated velocities. A problem in the present design of the AZPPT2 is in the oscillatory current patterns of the thruster circuit, characteristic of underdamped RLC circuits. This ringing poses problems to the lifetime of the capacitor and to the efficiency of the thruster. In this project, we have built a Rogowski coil to better characterize the current flow in the thruster and have modified the thruster to reduce the current ringing effect; the theory behind these efforts is also discussed. The results of this project are a Rogowski coil which measures current changes of 10^{10}A/s and sine wave frequencies of up to 6MHz and a diode module which reduced the reverse current by nearly 60%. Initial data suggest the specific impulse of the thruster will also be significantly increased by continued work in this area. Further advances are anticipated with improved diodes and shortened path length to the diodes for reduced inductance.

Christine McLeavey

Junior Paper: May 1, 2000

Advisor: Edgar Choueiri

Physics Advisor: Suzanne Staggs

with Tom Markusic and Bob Sorenson

I pledge my honor that I have not violated the Honor Code in writing this paper.

Contents

List of Figures

1 Introduction

The past 50 years have witnessed impressive growth in the new field of electric propulsion. Although the concept for an electric thruster existed half a century before, only in the late 1950s did the technology for sufficient electric power in space become available. An electric propulsion research program was begun in 1960 at NASA Lewis and at the Jet Propulsion Laboratory (Santarius [8]).

A major limitation on the implementation of some electric propulsion concepts is still the lack of high power supplies in space. Despite this, many research programs currently flourish, developing technology both for present and future spacecraft missions.

In this project, work has been done on the Ablative Z-Pinch Pulsed Plasma Thruster (AZPPT2), a type of electromagnetic thruster, aiming to minimize a current ringing problem in the circuit discharge. In the first section, we consider more carefully some of the advantages and applications of electric propulsion. In the following section, the AZPPT2 is examined and a physical model for the thruster firing is given. In section 3, the circuit ringing problem is presented in fuller detail; we show how one can model the thruster as a time-dependent inductor and resistor and how the limitation on the values of L, R, and C necessitate an underdamped circuit. In section 4, the proposed diode module is presented with justification for this design. In order to measure the current problem more accurately, a Rogowski coil was built; in section 5, the theory, design, and construction of the coil are described, along with the results. In section 6, the design and construction of the diode module is presented, followed again by the results. Finally, section 7 presents the conclusions drawn from this project.

2 Electric Propulsion

2.1 Characteristics and Applications

Although the rocket systems in use today demonstrate many different concepts of propulsion, the basic principle behind each is the same. By some method, fuel must be accelerated in a uniform direction and consequently discharged from the thruster. By Newton's third law, an impulse is imparted to the spacecraft equal and opposite that of the exhaust fuel.

Classic liquid propellant rockets involve chemical reactions which cause the fuel molecules to increase temperature and equivalently kinetic energy. The molecules are then directed outwards through careful design of the

geometry of the thruster nozzle. The resulting force, or thrust, ranges from .05 to 5×10^6 N (Wertz and Larson [10]). However, these systems are fundamentally limited by the particle speeds which can be achieved by the various chemical reactions and therefore require a significant fuel mass to produce a given thrust. The specific impulse, I_{sp}, is a measure of the amount of impulse that each unit weight of propellant gives to the spacecraft. It can be expressed mathematically, as is shown in Wertz and Larson [10] as

$$I_s = \frac{\int_0^t F dt}{g_o \int_0^t \dot{m} dt} \quad (1)$$

$$= \frac{F}{\dot{m} g_o} \quad (2)$$

with standard acceleration due to gravity g_o and the second equality holding if thrust F and mass loss $\dot{m}$ are constant. Specific impulse is related directly to the effective velocity of the propellant since $F = \frac{d}{dt} mv \approx \dot{m} v$.

Specific impulse is important as a means of quantifying the amount of fuel needed for various maneuvers. For example, as the orbit of an object is defined by the velocity at a given altitude, spacecraft adjustments are often measured by the change in velocity, $\triangle v$ required to change orbits. The amount of fuel needed to effect such a $\triangle v$ is given by the classic rocket equation,

$$m_p = m_o \left[1 - e^{-\frac{\triangle V}{I_{sp} g_o}} \right] \quad (3)$$

with propellant mass m_p and initial spacecraft mass m_o. Clearly, in order to minimize the required propellant mass, one must find a method of increasing specific impulse.

Electric Propulsion systems provide such an alternative. By accelerating ionized propellant through electric or magnetic fields, they are able to achieve much higher specific impulses. Typical I_{sp} for a liquid propellant thruster is 150-450s. With electric propulsion, I_{sp} can range anywhere from 300s for traditional Resistojet devices, which use I^2R power loss to heat the propellant and increase kinetic energy, to 5000s of certain electromagnetic devices which induce currents to flow through plasma (Wertz and Larson [10]). The latter capitalizes on the magnetic fields created by such current patterns, using them to accelerate the charged fuel particles to high velocities. The tradeoff, however, is twofold. The thrust produced by these systems is generally lower, ranging from 1μN to 2N. Also, the power and voltage requirements are significantly higher. At times, the mass saved from

fuel might be completely overwhelmed by the mass added for the increased power supply (Sutton [9]).

In addition to the benefits associated with the higher I_{sp} and consequently lower fuel mass, electric propulsion systems are also desirable because of their ability to create small, easily controlled impulse bits. A main problem with using traditional propulsion systems for attitude control and station keeping is that often times only small corrections are needed to fix the orientation of the vehicle. However, as most thrusters are only fully on or fully off, such small impulses would be impossible. An alternative to firing at less than full strength might be to fire at only a proportion of the time. One could digitize the amount of thrust demanded by the attitude control system and fire the thruster for a time proportional to the digital signal. Electric propulsion systems are especially compatible with such digital logic systems and are conducive to firing the brief, low thrust pulses needed for fine tuning of the spacecraft orientation.

Electric propulsion systems fill an important role in rocketry. Because of the high I_{sp}, they are beneficial to long term, interplanetary missions. The ability to fire small, controlled impulse bits also makes the method applicable to attitude control systems. The main drawbacks of these thrusters are generally in the potentially corrosive fuel used, in the lower thrusts generated, and in the high power supplies needed. The latter problem can be avoided by the use of a pulsed thruster, where a capacitor is charged to attain the needed voltage level and is discharged over a much shorter time to yield high power but only for a brief pulse.

2.2 Ablative Z-Pinch Pulsed Plasma Thruster

The Ablative Z-Pinch Pulsed Plasma Thruster (AZPPT2), now in its second design phase, possesses many of the advantages cited above. It is an electromagnetic system which utilizes a careful balance of electric and magnetic forces to accelerate the propellant. The geometry of the AZPPT2 is shown in Figure 1. A block of Teflon fuel sits between the anode and cathode, with a potential difference of 2kV between the two. The potential is established by a 38μF capacitor in parallel with the thruster, in turn charged by an external power supply. When a spark is initiated near the cathode, the surface layer of the Teflon ablates and molecules released from the surface become ionized. A gas with significant portions of electrons and ions is considered a plasma and demonstrates unique characteristics. Because the particles now interact through electromagnetic forces at greater distances due to their charge, the plasma will conduct current. In the case of the

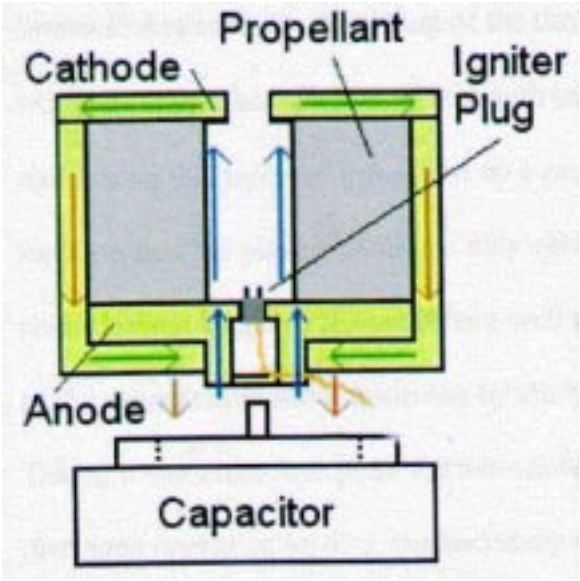

Figure 1: The geometry of the AZPPT2, as found in the work of Levine [7].

AZPPT2, the ablated Teflon creates a plasma that conducts current from cathode to anode.

As explained further in any Electricity and Magnetism text, such as Griffiths [3], the magnetic field surrounding an infinitely long wire carrying current I_1 in the $\hat{z}$ direction can be expressed in cylindrical coordinates as

$$\vec{B} = \frac{\mu_o I_1}{2\pi s}\hat{\phi} \tag{4}$$

with permittivity of free space μ_o, distance from the wire s, and $\hat{\phi}$ pointing circularly about the wire, according to the right hand rule.

The force per unit length on a second infinite wire, nearby and carrying current I_2 in the same direction is given by

$$\vec{f} = I_2\hat{z}\times\vec{B} \tag{5}$$

$$= -\frac{\mu_0 I_1 I_2}{2\pi s}\hat{s} \tag{6}$$

and causes the two wires to be attracted towards each other.

In a similar manner, as shown in Figure 2, one can consider the plasma as a set of parallel wires connecting cathode to anode. According to this last calculation, the wires attract each other. The plasma sheet contracts

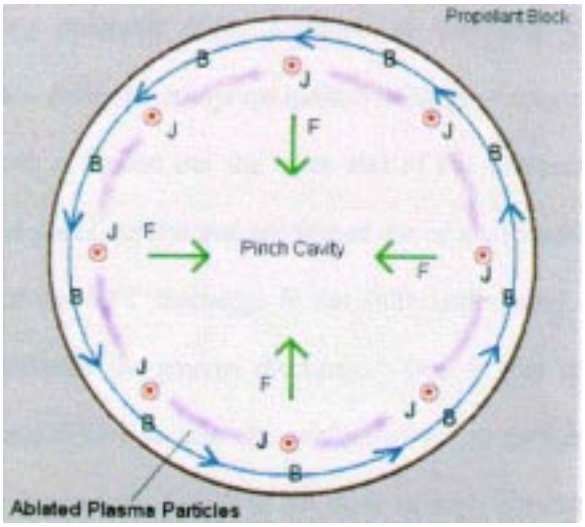

Figure 2: The ablated Teflon particles form a current conducting plasma inside the thruster. The current paths and corresponding magnetic fields are shown here in this figure from Levine [7].

to minimize distance between the parallel current paths. It has been experimentally determined that the current sheet progresses faster on the anode side and so the sheet reaches full contraction first at that end and then zips closed progressively towards the cathode (Levine [7]). Neutral and ionized Teflon molecules are expelled by this compressive thrust, in a sense much like a toothpaste container being squeezed from the bottom, as illustrated in Figure 3.

In previous testing of the AZPPT2, the impulse bit, equal to the impulse imparted per firing of the thruster, was found to be 2.870mN-s. Taking into account the mass ablation per shot, an I_{sp} of 468s was calculated. These numbers compared favorably with other pulsed plasma thruster (PPT) designs, especially given the fact that the thruster has a mass of only 2.5kg, measuring 16.3 cm in length and 8.9 cm in diameter (Levine [7]).

An additional advantage of the AZPPT2 is the small exit opening in the cathode. In many other PPT designs, propellant leaves the thruster after the main magnetic fields have already dissipated. The propellant then is not accelerated to high exhaust velocities and represents a major inefficiency in the I_{sp}, which measures thrust as a function of mass lost. Additionally, propellant is often a source of contamination to the spacecraft; stray Teflon particles might gradually coat sensitive parts of the spacecraft. The amount

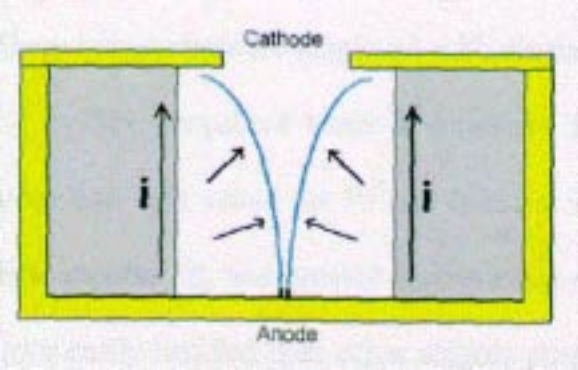

Figure 3: The magnetic forces of the AZPPT2 cause Teflon particles to be squeezed between the current sheets and directed out through the exhaust hole. Drawing from Levine [7]

of stray fuel leaving at low velocities should be minimized, as is done by the AZPPT2 configuration.

Because of its carefully controlled impulse bits, a major application for the AZPPT2 would be in making quick adjustments for attitude control on communications and other small satellites. Also, due to the high specific impulse, the thruster is a very efficient way of minimizing the fuel mass required on a spacecraft. The thruster could be used for orbit transfers, as long as low thrusts and consequently slow orbit transfers were acceptable.

Additional applications of the thruster which are currently being explored are its potential use in depositing fine layers of Teflon and in providing a source of X-rays for lithography.

3 Circuit Analysis

One major problem with the thruster, which is a general problem with pulsed plasma thrusters, is an effect known as current ringing. In this section, we will consider the thruster as a time-varying inductive and resistive load in an RLC circuit and will find that the circuit is necessarily underdamped. There are two main problems associated with this. First, the capacitor is designed so that the external casing should be positive with respect to the internal lead. Reversing the polarity severely degrades the lifetime of the capacitor, which is a major issue for any component to be flown in space. Additionally, the AZPPT2 has been shown to be less efficient if charged and fired with the anode and cathode reversed (Levine [7]).

The resistance of the AZPPT2 is inversely proportional to the conductivity of the plasma, varying with the number of charged particles in the chamber. The self-inductance L can be seen from a derivation following that in *Physics of Electric Propulsion* by Robert Jahn [6], beginning with the relation

$$\Phi = LI \tag{7}$$

for current I and magnetic flux Φ through the current loop of the thruster circuit, equal to $\int \vec{B} \cdot d\vec{A}$ for magnetic field $\vec{B}$ and element of area $d\vec{A}$.

From Maxwell's law in integral form, one writes

$$\int \vec{E} \cdot d\vec{l} = -\frac{d}{dt} \int \vec{B} \cdot d\vec{a} = -\dot{\Phi} \tag{8}$$

$$-V + IR = -\frac{d}{dt}(LI) \tag{9}$$

$$= -L\dot{I} - I\dot{L} \tag{10}$$

for voltage V across the capacitor.

From this, one can determine the power transferred as energy is moved from the $\frac{1}{2}CV^2$ stored at the capacitor to be dissipated by the resistance and to increase the inductance of the loop. Power P is simply IV and can be integrated over time to determine the work done, W.

$$W = \int_0^\tau I(IR + L\dot{I} + I\dot{L})dt \tag{11}$$

$$= \int_0^\tau (I^2R + \frac{d}{dt}(\frac{1}{2}LI^2) + \frac{1}{2}I^2\dot{L})dt \tag{12}$$

$$= \int_0^\tau (I^2R + \frac{1}{2}I^2\dot{L})dt \tag{13}$$

where the final equation is found by noting that the current I is zero at $t = 0$ and $t = \tau$. The first term reflects thermal loss in the circuit while the second is a measure, although idealized, of the kinetic energy transferred to the plasma. As we will see shortly, the change in inductance L is directly due to the motion of the current sheet. Since the available work is fixed by the energy initially stored in the capacitor, it is of interest to attempt to maximize the change in inductance. One would then hope that $\dot{L}$ is at least of equal if not greater magnitude than R.

Jahn continues to analyze the case of a parallel plate accelerator geometry. However, $\dot{L}$ can also be estimated for the z-pinch configuration. As the current sheet moves, the area of the circuit increases so that inductance

also increases. Returning to the image of n parallel wires instead of a sheet of plasma, one can consider the case where each wire moves from the edge of the Teflon directly to the center of the thruster. Assuming that n is large and therefore that the approximation of the many wires as a sheet of plasma is good, one can use Ampere's Law to express the magnetic field at distance s from the center axis with the sheet at distance s_o from the axis as

$$\vec{B} = \begin{cases} 0 & \text{if } s < s_o \\ \frac{\mu_o I}{2\pi s}\hat{\phi} & \text{otherwise} \end{cases} \tag{14}$$

where I is the total current through the thruster and $\hat{\phi}$ circles the center axis. The increase in area of the enclosed loop is simply rh where r is the distance the wire moves and h is the length between anode and cathode. Taking the thruster dimensions $r = 1.3$cm and $h = 4.0$cm, this is then an increase of 5.1cm^2. One can express the change in inductance L of the n^{th} wire as

$$\begin{aligned} \triangle L_n &= \triangle\frac{\Phi}{I_n} && (15)\\ &= \frac{I_n\triangle\Phi - \Phi\triangle I_n}{I_n^2} && (16)\\ &\approx \frac{\triangle\Phi}{I_n} && (17) \end{aligned}$$

where I_n is the current in the n^{th} wire, equal to I/n. The second line is obtained through the assumption that the current magnitude is established relatively early and does not change significantly as the wires move inward. From this, the change in inductance is

$$\begin{aligned} \triangle L_n &= \frac{\mu_o I}{2\pi I_n}\int_0^r \frac{hs\,ds}{s} && (18)\\ &= \frac{\mu_o n r h}{2\pi} && (19)\\ &\approx n \times 10^{-10} H && (20) \end{aligned}$$

The inductance of n parallel inductors is simply the sum of their inverses, so $L = (\frac{1}{L_n} + \frac{1}{L_n} + \cdots)^{-1} = \frac{L_n}{n}$. The change in inductance of the entire circuit is then 10^{-10}H. If one takes a standard discharge time on the order of 1μs, this would imply an average $\dot{L}$ of $10^{-4}\Omega$.

The energy imparted to the current sheet is also fundamentally limited by the magnitude of the current. At a given moment in time, the energy

stored in the inductor is $\frac{1}{2}LI^2$. Imagining that all energy stored in the capacitor was transferred to the inductor and noting that the inductance monotonically increases during the discharge, the largest possible current is then $I_{max} = \sqrt{CV^2/L_o}$ for initial inductance L_o. As the actual energy transferred to the current sheet is

$$W_o = \int_0^\tau \frac{1}{2} I^2 \dot{L} dt < I_{max}^2 \int_o^\tau \dot{L} dt = I_{max}^2 \triangle L \tag{21}$$

For a reasonable efficiency, one would look for $\triangle L$ and L_o to be of the same order of magnitude. From the derivation above, it would seem an L_o of 100pH would be appropriate. However, from fitting curves of actual thruster shots, values for R and L of 50mΩ and 100nH, respectively, were chosen, indicating that the above derivation must underestimate the increase in magnetic flux causing an exceedingly low $\triangle L$. The above work includes only geometrical considerations and entirely neglects the dynamics of the nature of the plasma and so could be missing variables due to the changing physical conditions which might affect the overall inductance. The important point is that L and R must not be too large in order to preserve thruster efficiency.

With limitations on L and R set, one can now proceed to consider the full thruster circuit. The circuit is simple, with a resistor, charged capacitor, and inductor in series at time $t = 0$. Setting net voltage around a circuit loop equal to zero, one derives the relation

$$L_o \ddot{Q} + R_o \dot{Q} + \frac{Q}{C} = 0 \tag{22}$$

with Q referring to charge on the positive plate of the capacitor. With the initial conditions $Q = Q_o$ and $I = 0$, one has the usual case of three possible behaviors. For $C > 4L_o/R_o^2$ the circuit is overdamped, for $C < 4L_o/R_o^2$, it is underdamped, and at equality, critical damping is achieved.

With $L = 10^{-10}$H and $R = .0001\Omega$, critical damping would occur at $C_{crit} = .04$F. With the more realistic $L = 10^{-7}$H and $R = 50\text{m}\Omega$, $C_{crit} = 160\mu$F. Even were these values technically feasible for small space-qualified capacitors, the time constant for the capacitor to discharge would be enormous and not condusive to the large currents needed to run the thruster. In practice, the capacitor on the AZPPT2 is 38μF. The circuit displays a current ringing pattern, as is shown in Figure 4.

As noted previously, the ringing is an undesirable effect. The focus of this project was to reduce this problem, thereby increasing thruster efficiency and improving capacitor lifetime. The first main focus was to develop a probe for

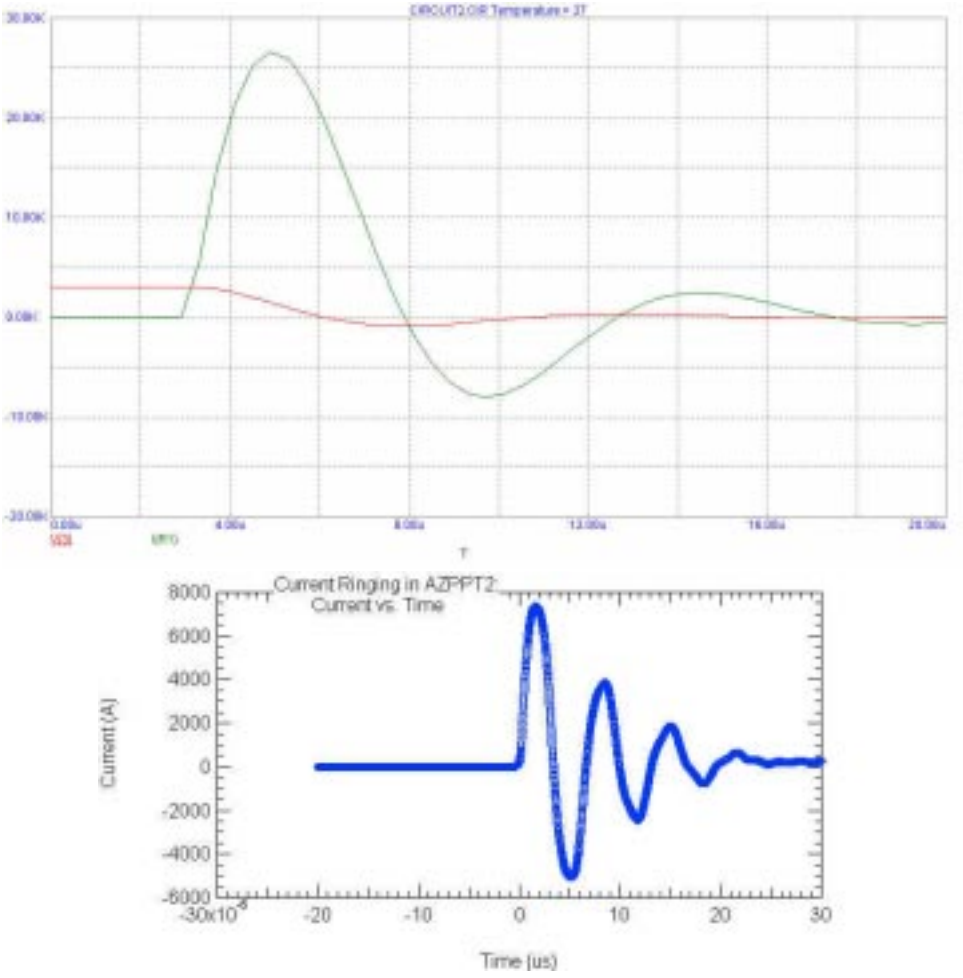

Figure 4: The current ringing problem is shown in the top graph according to a Spice simulation (Bello [1]) with the thruster modeled as a 50mΩ resistor in series with a 100nH inductor. The circuit used for the simulation is a simple RLC circuit with the three elements in series and a switch used to close the circuit after the 38μF capacitor is initialized with a voltage of 2kV. The traces shown are the transient reponses of the current and voltage across the capacitor. The second graph shows the output of the Rogowski coil from a typical shot of the unmodified thruster, as integrated with IgorPro [4].

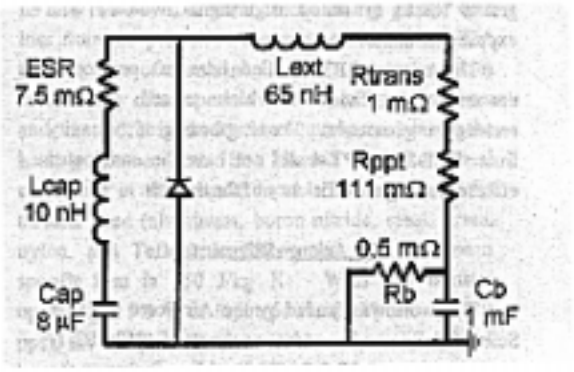

Figure 5: The new circuit would add a diode in parallel with the charging capacitor, in order to provide a secondary path for current flow during the discharge. Burton and Turchi [2].

dynamically measuring the current at any point within the thruster circuit. The second was to work on implementing a new design, as discussed in the next section, aimed at minimizing current ringing.

4 Proposed Configuration, with Diodes

Current flows from the positive end of the capacitor, through the resistance and inductance of the thruster, and builds up on the negative side of the capacitor. If an alternative route could be provided to the current once the voltage across the capacitor was neutralized, then the reverse charging of the capacitor would not occur. A method of achieving this was suggested in a report by Burton and Turchi [2]. The proposed circuit is shown in Figure 5.

When the voltage across the capacitor becomes negative, the diode becomes forward biased and current is allowed to flow. Charge will no longer build up on the capacitor, but will cycle back through the diode and to the thruster, remaining in the ideal voltage configuration. Eventually, all energy will be dissipated through the movement of the current sheet and the accompanying acceleration of the propellant, and through the heat loss from the resistance in the circuit.

Although the switching time of the diode is on the order of nanoseconds and certainly fast enough for this application, a delay is incurred due to the inductance of the path leading to and from the diode. The main problem, however, is in finding diodes capable of handling such currents.

The requirements on the diode in the circuit are extreme. Not only must it hold off a reverse voltage of 2kV, but it must allow forward currents on the order of 10kA for pulses of several microsecond durations. Additionally, the module must be small enough to fit conveniently on the thruster. A main feature of the AZPPT2 is its small size and weight, which must not be compromised by overly large diodes.

In order to meet these requirements, it was necessary to employ two diodes in series, each holding off only 1kV. Additionally, four diode pairs were used, rather than a single path, in order to reduce the current traveling through any single diode and to reduce the inductance, which adds inversely when in parallel. In order to insure that each diode would see only 1kV, despite inequalities in the construction of the diodes, a voltage divider was added. The leakage current of the diodes was determined and then resistors were chosen to allow 10 times that leakage current. This insured that the voltage at the junction at the midpoint of the diode pairs was effectively 1kV.

The final proposed circuit is shown in Figure 6. The diodes chosen were the International Rectifier Fast Recovery Rectifiers, part 85HFL100S05 [5]. A Spice simulation of this new configuration as shown in the figure was run to find the current and voltage curves which result from the firing of the thruster. For these purposes, the thruster was modeled as a 100nH inductor in series with a 50mΩ resistor. To establish the initial conditions, the 38μF capacitor was considered to be charged to 2kV. Then, Switch2 was closed and the transient voltage and current across the capacitor were determined as functions of time. The results of this simulation are shown in Figure 7

5 Rogowski Coil

5.1 Theory

In order to make improvements on the current patterns in the thruster circuit, it was first necessary to determine an accurate method of measuring current. The Rogowski coil is a surprisingly simple application of Maxwell's equations for electromagnetism. It is basically a torus with a wire looped around the entire main circumference, as in the photograph in Figure 8. With the eventual goal of measuring current I as a function of time t, the coil instead measures $\frac{dI}{dt}$ by reacting to the corresponding changing magnetic field, as will be discussed. The voltage output from the coil is then numerically integrated to provide the desired $I(t)$. Following a derivation given in Wright [11], one uses Ampere's Law to express the magnetic field

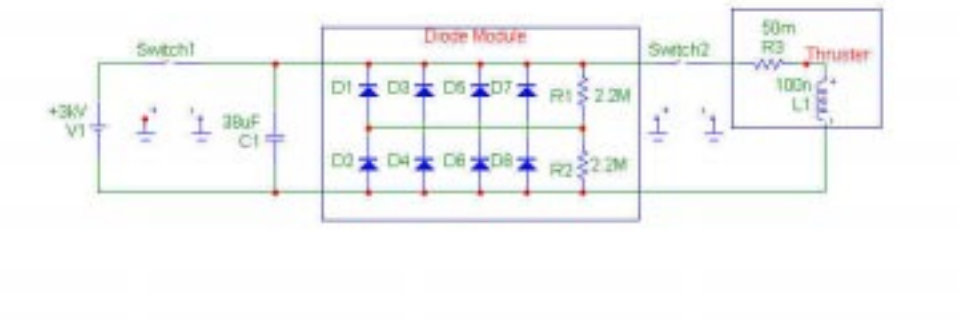

Figure 6: The diode module circuit; eight diodes are used because of the physical constraints of the available diodes.

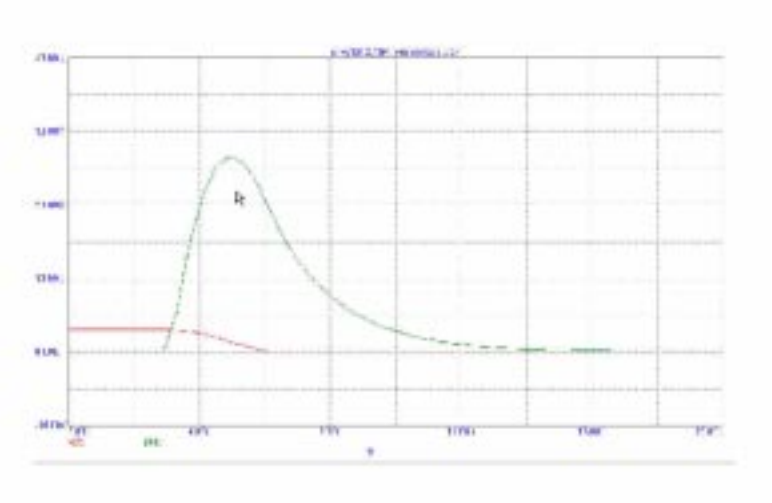

Figure 7: A Spice simulation of the thruster circuitry with diodes installed.

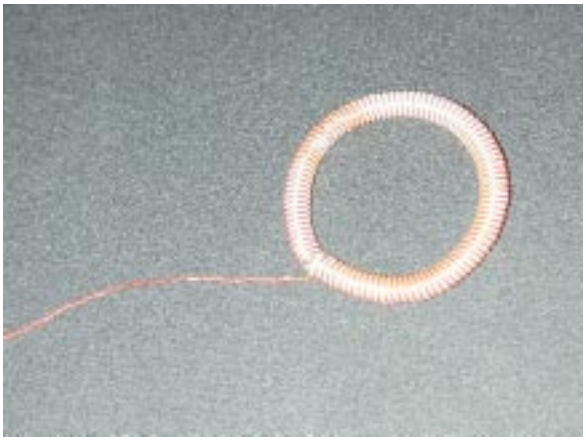

Figure 8: A photograph of the finished Rogowski coil.

$\vec{B}$ around an enclosed current I_{enc} as

$$\int \vec{B} \cdot d\vec{l} \quad = \quad \mu_o I_{enc} \tag{23}$$

with μ_o as the permeability of free space, equal to $4\pi \times 10^{-7}$ H/m.

If the magnetic field fluctuates, it produces an electric field, according to Faraday's Law,

$$\vec{\nabla} \times \vec{E} \quad = \quad -\frac{\partial B}{\partial t} \tag{24}$$

Using Stokes' Law, this can be expressed in integral form in terms of the magnetic flux $\Phi = \int \vec{B} \cdot d\vec{a}$:

$$V = \int \vec{E} \cdot d\vec{l} = -\frac{d\Phi}{dt} \tag{25}$$

Here, V is the electromagnetic force, the voltage induced around a complete loop.

The next step is to express these quantities in terms of the N loops of the Rogowski coil. Then, the net magnetic flux, assuming that $\vec{B}$ is a constant and in a direction circling I_{enc} is

$$\Phi \quad = \quad NBA \tag{26}$$

for cross-sectional area A. Differentiating Eq. 26 and using Eq. 25 to solve for B, one finds

$$\frac{\partial B}{\partial t} \quad = \quad -\frac{1}{NA} V(t) \tag{27}$$

Referring back to Eq. 23, one expresses the changing current as

$$\frac{dI}{dt} = \frac{1}{\mu_o}\int \frac{\partial \vec{B}}{\partial t}\cdot d\vec{l} \quad (28)$$

$$= \frac{1}{\mu_o} L \frac{\partial B}{\partial t} \quad (29)$$

$$= \frac{L}{\mu_o N A} V(t) \quad (30)$$

so that

$$I(t) = \frac{L}{\mu_o N A}\int_0^t V(t')dt'. \quad (31)$$

In this derivation, no assumption has been made regarding the placement of the current flowing through Rogowski coil. Theoretically, the location of the current is insignificant; current flowing inside will be detected while current flowing outside will have no effect. In practice, there will be some effect due to imperfections in the construction of the coil and limitations in connecting the torus back upon itself. This problem can be minimized through careful design of the coil and is not a major source of error for this application as the current to be detected in the thruster all flows through the center of the loop.

5.2 Construction

Three separate Rogowski coils were constructed, each of different sensitivity as the amount of current and rate of change of current in the thruster were known only within a few orders of magnitude. The first resulted in an output voltage range of $\pm$500V, too high for practical use. The second was rejected because it was considered less symmetrically constructed than the others. The third produced an output voltage range of $\pm$150V and was chosen for subsequent use.

The first design decision lay in choosing a core for the coil, around which the wire would be wrapped in loops. Symmetry of the loops was an important consideration in order to be able to measure a current passing through the coil regardless of its position inside the coil. Because of this, a threaded 10-24 nylon piece, with cross-sectional area .14cm^2 and 101 loops was chosen. This corresponded to a length $L = 10.7$cm, which was bent into a circle of diameter 3.4cm by heating with an electric blower.

A wire was led first around the main circle, and then looped back upon itself, following the threads in the nylon. The final coil was then covered with Q-dope to fix the wires and to provide electrical insulation.

Because the coil would need to output high frequency signals, it was important to match the impedance to that of the BNC cable and the final oscilloscope. The resistance of the loop was calculated from the known resistance per length of the wire and was found to be .5Ω. The inductance of the loop was measured by connecting the loop in series with various capacitors. A series LC circuit has a complex impedance of $Z = \frac{1}{i\omega C} + i\omega L = i(\omega^2 LC - 1)/\omega C$. At the resonant frequency, an input sine wave would effectively see a short circuit. Therefore, the resonant frequency could be found by measuring the frequency at which current through the circuit was a maximum. From this, the inductance of the first coil was found to be $1.7 \pm .3 \mu$H.

The BNC cable and the oscilloscope both had impedances of 50Ω and so in order to match this, a 49.5Ω resistor was added in series at the end of one lead of the coil. The inductance and stray capacitance of the coil, the latter measured with a capacitance meter to be 10pF between the coil and ground, were too small to significantly affect the impedance matching.

From Eq. 31, one would expect the relationship

$$I(t) = (6.15 \times 10^6 \Omega^{-1} s^{-1}) \int_0^t V(t')dt'. \tag{32}$$

Therefore, a $\frac{dI}{dt}$ on the order of 10^9A/s, as was expected at the time, would give an output on the order of 100V. Although large, there was also the consideration that the coil would not necessarily output as large a voltage as theoretically predicted as the model used was an idealized version that took nothing into account of the physical materials used.

Further calibration was performed by placing a wire through the loop and varying the frequency of a sine wave current passing through the wire. Since the amplitude of the current remained a constant $1.05 \pm .02$A, peak-to-peak, the relationship between input current and output voltage of the coil was simply

$$V = a\frac{dI}{dt} = aI_o(2\pi f)cos(2\pi f t), \tag{33}$$

where a is a constant of proportionality to be determined from the slope of V_{max} versus f. From this, it was determined that a 10^9A/s input current change would produce an output voltage of ±25V. However, when the first coil was tested in the thruster, it produced an output voltage range of ±500V, indicating that the current change was much higher than initially estimated. The 49.5Ω resistor was the first piece damaged; in order to remedy this and to protect the oscilloscope, the coil was redesigned.

The second coil was constructed simply by taking a wire and wrapping it back around itself, using the thickness of the wire insulation as the core diameter. The coil performed well in the tests to determine self-inductance and in calibration. However, it was rejected due to doubts regarding the symmetry of the loops and because of the inconveniently large size of the coil leads.

A final coil was based more similarly on the model of the initial one. This time, a thinner nylon cord, with cross-sectional area .9cm^2, was used. Additionally, every other thread was skipped, so that even with the closer threads of the new cord, the number of loops was reduced to 78. The length of the coil was 10.0cm and it was bent into a circle of diameter 3.2cm. By the same testing methods, the inductance was determined to be $6\pm.5\mu$H. A calibration was performed and the graph of output voltage as a function of input frequency is shown in Figure 9. The output voltage clearly begins to decline as frequencies of 6MHz are reached. However, as the main thruster ringing occurs at a main frequency on the order of 800KHz, this is an acceptable margin. Using a best fit line for the data points below a frequency of 2MHz, one finds the constant of proportionality a in Eq. 33 to be $1.4\times10^{-8} \pm 10^{-9}\Omega^{-1}s^{-1}$. An error of 5% is estimated to account for the limited frequency range over which this constant is determined, even though the line fit itself is more accurate. From this, one would expect a $\frac{dI}{dt}$ of 10^{10}A/s to produce an output voltage of 140V. This value, while still large, is manageable with a sturdier 50Ω resistor. Physical difficulties in creating a symmetric coil with fewer loops and smaller cross-sectional area precluded attempting to further decrease the magnitude of the voltage response. Although for a continuous current, this voltage level would require a resistor with a power rating of nearly 400W, for this quick pulse application, there is not enough time for significant heating to occur and the only resistor requirement is to hold off 140V without shorting.

The coil was then tested inside the thruster. The results are shown and discussed in the following section.

5.3 Results

The third Rogowski coil succeeded in providing a useful output signal upon testing. It was placed in the space in between the capacitor top and the thruster bottom. In this orientation, the current measured is that leading directly from the negative side of the capacitor to the anode; this current is proportional to the changing voltage of the capacitor. Other currents in the circuit that would be less directly accessible through other means, such as

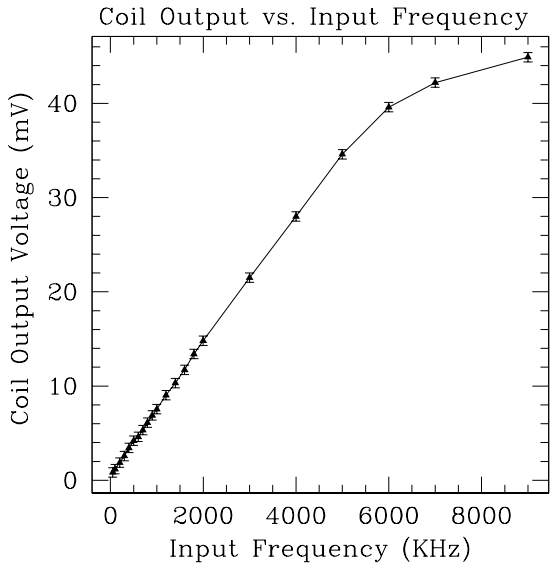

Figure 9: Output voltage of the Rogowski coil is shown as a function of input frequency for a sine wave current of constant peak-to-peak amplitude 1.05±.02 A.

those passing through the diodes, could also be measured by the coil.

The output of the coil is sent to a digital oscilloscope and then downloaded into IgorPro for data analysis. The integrated output signal following a typical shot of the thruster was shown earlier in Figure 4.

6 Diode Module

6.1 Construction

Included in the appendix are drawings of the diodes and a photograph of the diode module. Since each individual diode could only hold off a maximum of 1kV reverse bias voltage, it was necessary to put two in series to support the full 2kV. Each diode had a small reverse leakage current, corresponding to a high resistance. Ideally, the resistances would be matched and the voltage across one diode would be exactly one-half that of the voltage across the two, as it would be in the case of a normal voltage divider constructed of two matched resisters. However, in practice, this balance can not be guaranteed. The diodes were each tested by connected them across a 850V

reverse voltage. The current through the diodes was measured and was found to be on average 9μA and in the worst case 12μA, indicating a lowest resistance of 71MΩ. In order to insure a more even voltage division, two $2.25\pm.01$MΩ, 2W resistors were placed in series across the 2kV, with the junction between the two connected to the junction between the diode pairs, as was indicated in Figure 6. These resistors allow a leakage current of .88mA, enough to fully define the voltage at the midpoint of the diodes, yet not so large as to significantly affect the amount of time needed to charge the capacitors.

A flat circular ring was machined out of Aluminum with inside and outside diameters of 2.5" and 4.5", respectively. A set of four diodes led from the positive side of the capacitor to the middle of the metal ring, while four more diodes connected from the outside of the ring to lead wires which ran directly to the anode of the thruster. The resistors were connected across one of the diode pairs; since their application was in steady state voltage balancing, their exact placement was not crucial. The design of the diode pairs focused on attempting to minimize inductance in the current paths. The four diode pairs were spaced symmetrically around the ring.

The diode module was designed to fit directly onto the back of the capacitor. It was held in place by a hose clamp.

6.2 Results

The current pattern of a typical thruster shot with the diode module is shown superimposed over a shot from the original, unmodified thruster in Figure 10. The reverse current is reduced to a peak of 2100A, markedly less than the original 5000A, signifying that the reverse voltage on the capacitor must also be decreased, according to $V_c = V_o - \frac{1}{C}\int I dt$.

Because the experiment was to be run in vacuum, parts at differing voltages of up to 2kV were placed only 1/8" apart, knowing that the difficulty in causing a current to arc through a vacuum would prevent any problems. Before the implementation of the device, there was concern that gas expelled from the thruster shots might migrate back towards the diode module and cause a short across the 2kV. Fortunately, this did not become a problem when testing was performed.

Although the current reversal was reduced, it is still present. Two main problems presented themselves in this implementation. The first was that the path the current would follow through the diodes is still of significant length. At these switching times, even wires must be considered as having non-zero inductance; the path length presented a significant impedance

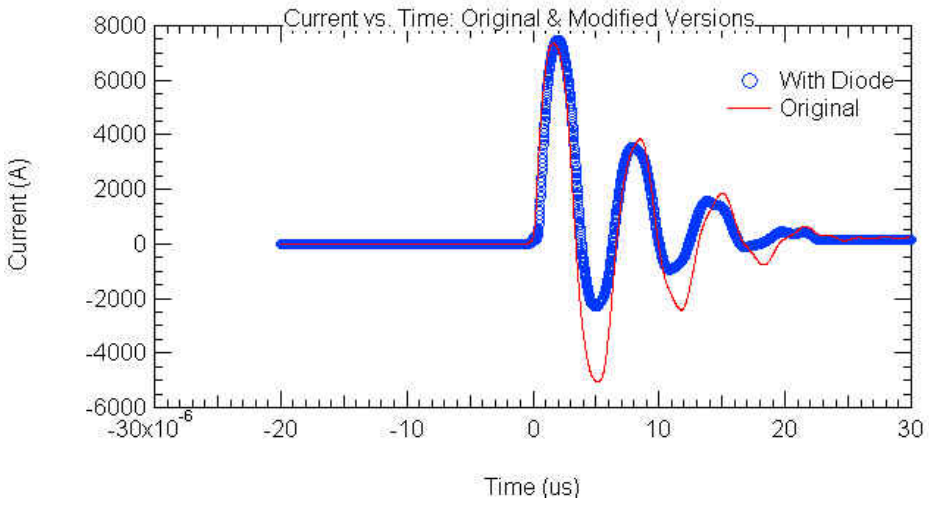

Figure 10: The current pattern from the new thruster is shown in comparison with a typical shot from the unmodified version.

discouraging current to flow through the diodes rather than to the capacitor.

A second more major problem was in the physical limitations of the diodes. As few diodes are rated for the brief pulses of currents present in this application, maximal values for It and I^2t were extrapolated from the curves in the data sheets. With four diodes in parallel, it was thought that the current tolerances would be large enough. However, in the course of the testing, five of the eight diodes were compromised, clearly surpassing their capabilities for conducting current. This would also suggest a reason why the current reversal problem was not solved by these diodes; the diodes simply could not conduct enough current to prevent the capacitor from reverse charging.

New diodes have been ordered, though at several times the cost, weight, and size of the original ones. Testing with these new diodes will proceed in the next few weeks and increased improvements in minimizing the current reversal are expected.

Because the diodes were damaged after the first shot, it was difficult to obtain any information about the impulse bit and specific impulse of the modified thruster. However, from the one data point available, the only time the diodes were still certainly intact, the impulse bit was determined to be .0026 Ns. It was clearly impossible to measure the mass loss from this single shot; the difference in the mass of the Teflon fuel block before and after the

shot is beyond the resolution of the balance. Still, it is possible to use data from previous tests of multiple firings with the original thruster, in which a mass per shot value of 3.17×10^{-7}kg was determined. Use of this number led to a calculated I_{sp} of 834s, a figure 165% those found in the latest tests without the diodes. Although no conclusions can reasonably be drawn from this single point, it does indicate the possibility for major improvements in thruster performance, should such measurements be repeatable with the new diodes.

7 Conclusion

Although the current ringing problem still exists, the magnitude of the reverse current has been reduced by a factor of 58% from the original value. With the first diodes chosen, the current flow exceeded their ratings, leading to a breakdown in the devices. Results suggest that the plan to use diodes will be effective, but only if a hardier model can be employed. New diodes with higher current conduction capabilities are to be tested and are expected to further improve performance, both in reducing the ringing and possibly also in increasing specific impulse.

Three Rogowski coils were built in the process of this project. Although only the third is of a suitable range for use in measuring current through the thruster, the others are calibrated and would be applicable to measuring current through a single diode, or to other projects that would require current measurements. The coils are limited by an upper cutoff frequency of approximately 6MHz. However, this is not a major problem for this application as the current ringing here is of the order of 800 KHz.

References

[1] Bello, Vincent B. "SPICE Simulations Home Page," April 1999. http://members.aol.com/DrVGB/

[2] Burton, R.L. and Turchi, P.J. "Pulsed Plasma Thruster." Journal of Propulsion and Power, Vol 14., No. 5. Sept-Oct 1998.

[3] Griffiths, David J. *Introduction to Electrodynamics, 2nd Ed.* New Jersey: Prentice Hall, 1989.

[4] IgorPro. http://www.wavemetrics.com/

[5] International Rectifier Data Sheet No. PD-2.093.

[6] Jahn, Robert G. *Physics of Electric Propulsion.* New York: McGraw-Hill Book Co., 1968.

[7] Levine, Joshua Z. "Ablative Z-Pinch Pulsed Plasma Thruster." Final Report for Undergraduate Independent Work for the Princeton University Department of Mechanical and Aerospace Engineering, 2000.

[8] Santarius, John F. "Plasma and Electric Propulsion," July 1998. http://rigel.neep.wisc.edu/ jfs/neep602.lect31.97/plasmaProp.html

[9] Sutton, George P. *Rocket Propulsion Elements: An Introduction to the Engineering of Rockets, 6th Ed.* New York: John Wiley & Sons, Inc., 1992.

[10] Wertz, James R. and Larson, Wiley J., ed. *Space Mission Analysis and Design, 3rd Ed.* Boston: Kluwer Academic Pulblishers, 1999.

[11] Wright, Edward S., Jahn, Robert G. and von Jaskowsky, Woldemar F. "The Design and Development of Rogowski Coil Probes for Measurement of Current Density Distribution in a Plasma Pinch." Princeton University Department of Aerospace and Mechanical Sciences: Princeton, NJ, 1965. NASA Report No. 740.

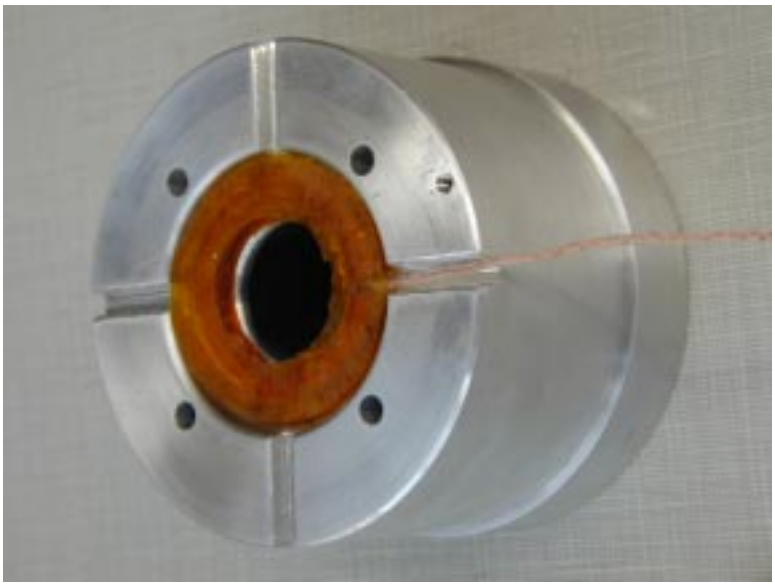

Figure 11: The Rogowski coil photographed in part of the thruster.

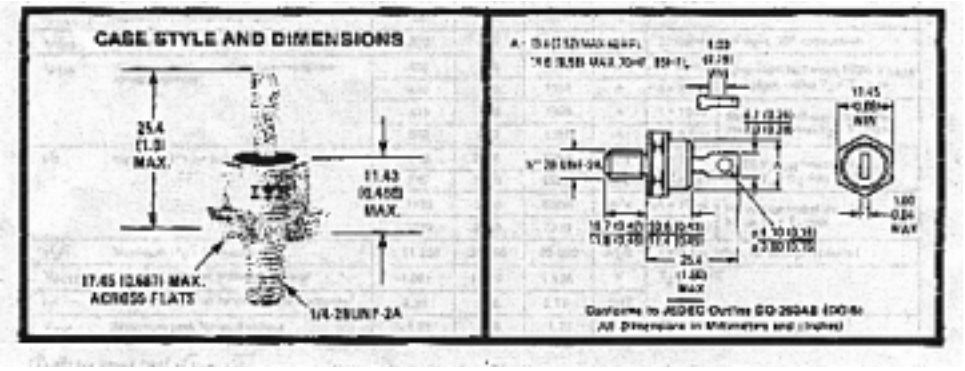

Figure 12: The physical case of the 85HFL100S05 diode. From the International Rectifier data sheet [5].

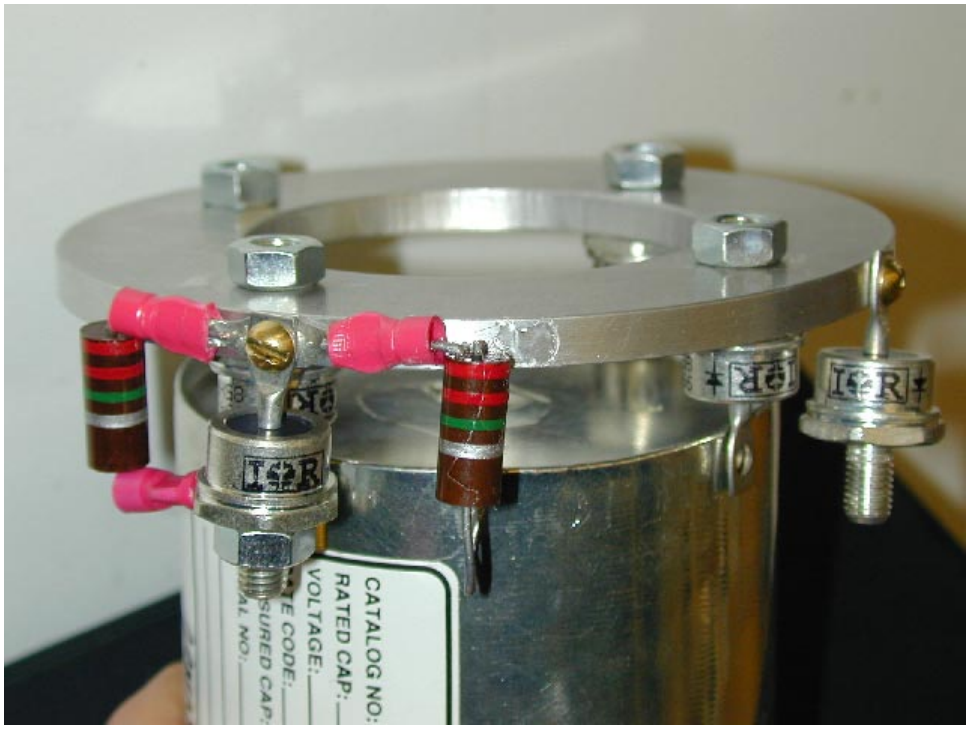

Figure 13: A photograph of the completed diode module.